Supporting Information

Green and Facile Fabrication of Hollow Porous MnO/C Microspheres from Microalgaes for Lithium-Ion Batteries

Yang Xia,[†] Zhen Xiao,[‡] Xiao Dou,[†] Hui Huang,[†] Xianghong Lu,[†] Rongjun Yan,[†] Yongping Gan,[†] Wenjun Zhu,[†] Jiangping Tu,[‡] Wenkui Zhang,[†,*] and Xinyong Tao[†,*]

[†]*College of Chemical Engineering and Materials Science, Zhejiang University of Technology, Hangzhou 310014, People's Republic of China*

[‡]*Department of Materials Science and Engineering, Zhejiang University, Hangzhou 310027, People's Republic of China*

Address correspondence to msechem@zjut.edu.cn, tao@zjut.edu.cn.

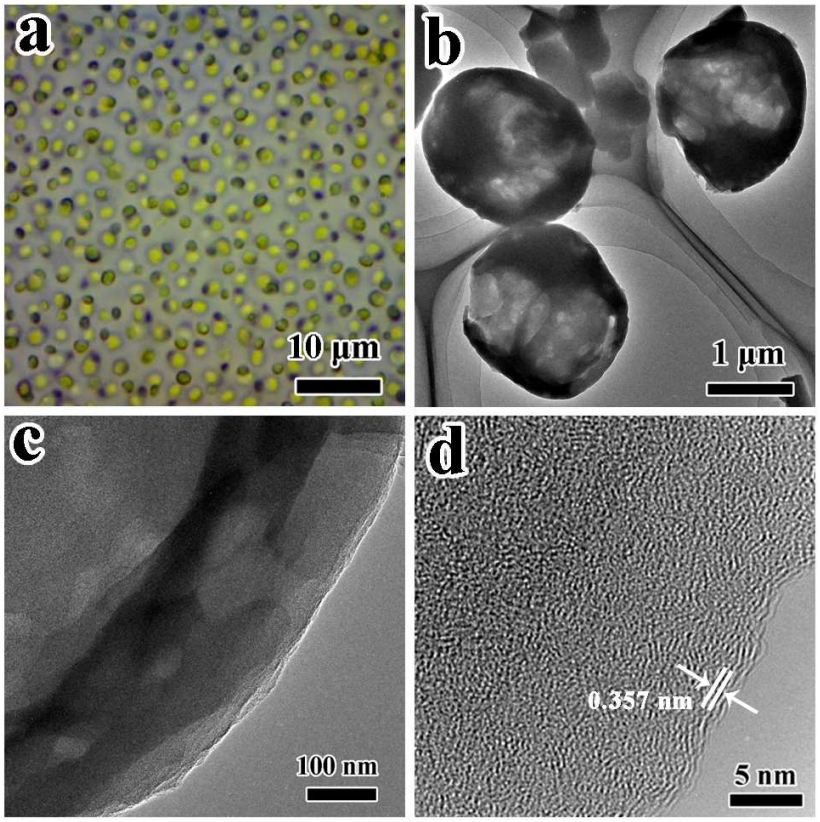

Figure S1. (a) The optical microscope image of living *N. oculata*; (b)-(c) TEM images of the carbon residues of *N. oculata*; (d) The HRTEM image of the carbon residues of *N. oculata*.

As shown in Figure S1a, *N. oculata* is a sphere-shaped algae with a uniform size of 2 μm in diameter. After the calcination, as shown in Figure S1b, the carbon residues of *N. oculata* exhibit the similar size and morphology to the original ones. The hollow and porous microstructure can also be revealed by the sharp contrast between shell and interior from Figure S1c. The 0.357 nm interval of the lattice fringes detected in Figure S1d indicates that *N. oculata* has successfully transformed to carbon. Therefore, *N. oculata* used in this work will play multiple roles (biotemplates and carbon sources), and can easily evolve a hollow and porous carbon microsphere.

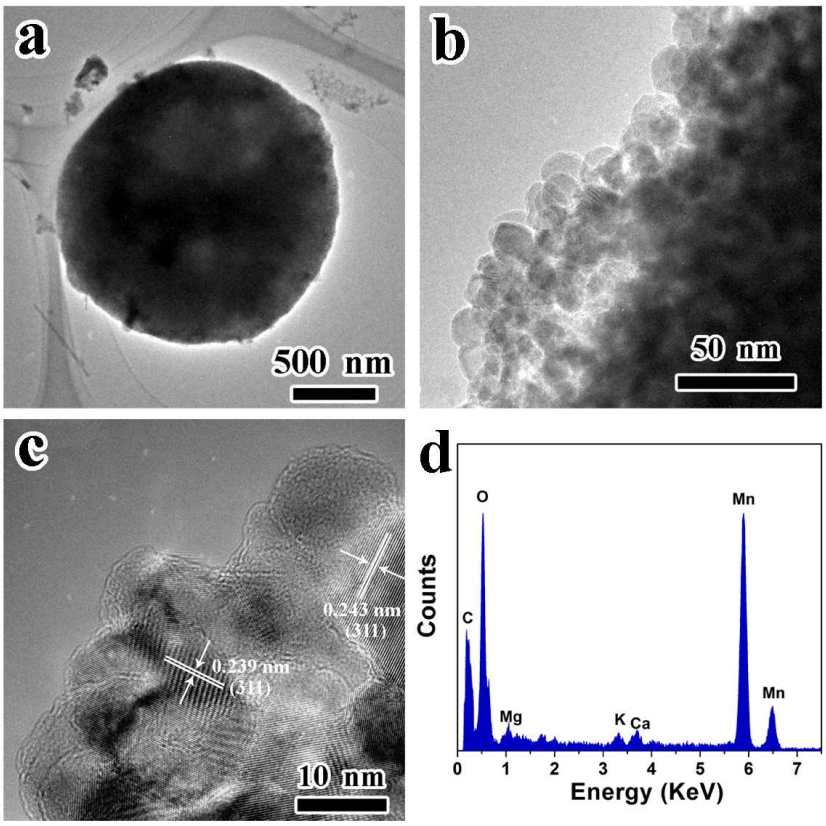

Figure S2. (a)-(b) The TEM images of the sample without PS coatings; (c) HRTEM image of the sample without PS coatings; (d) The corresponding EDS results.

Figure S2a displays that the sample without PS coating has the similar size to *N. oculata* biotemplates and the sample with PS coating. However, after a carful observation, it can be seen that nanocrystals are attached to each other on the surface of microsphere (Figure S2b). HRTEM image (Figure S2c) also confirms the polycrystalline character. In addition, there is no obvious carbon layer on the surface of the sample, which is different from the sample with PS coating. The measured fringe spacing values are about 0.243 and 0.239 nm, matching well with (311) planes of MnO_2. EDS results (Figure S2d) further demonstrate that the main elements in the sample without PS coating are C, Mn and O. The trace elements (such as Mg, Ca and K) also can be found, which is similar to the sample coating PS.

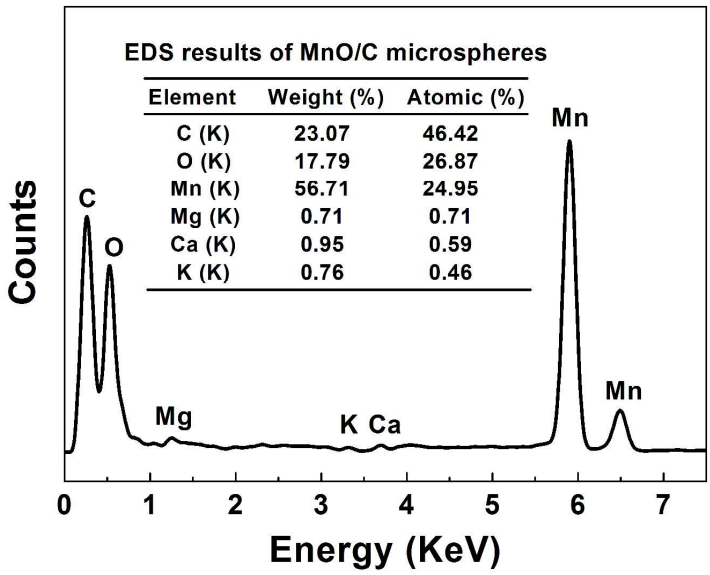

Figure S3. EDS spectrum of MnO/C microspheres. The inset is the corresponding EDS results taken from 5 different regions and calculated from the average values.

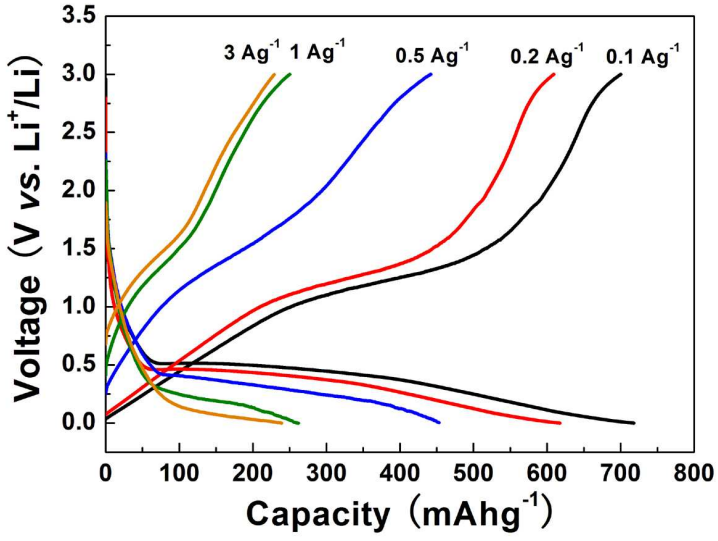

Figure S4. The discharge-charge curves of MnO/C electrodes at different current densities.

Table S1 Comparison of BET specific surface area and BJH pore size distribution of various MnO based anode materials

Samples	BET specific surface area (m^2g^{-1})	pore distribution (nm)	Ref.
Porous MnO/C nanotubes	40	7.7	10
MnO@1-D carbon composites	64	24.57	11
MnO@carbon core-shell nanowires	6.86	13.2	14
Porous C-MnO disks	75.3	20	15
Mesoporous MnO/C Networks	82.7	2.8/7.6	16
Hierarchical Micro/Nanostructured MnO	52.5	20/60	17
MnO/graphite nanosheet	58.1	-	19
Hollow porous MnO/C microspheres	76.9	11/87	This work

Table S2 Comparison of the electrochemical performances of various MnO anode materials

Samples	Current density ($mA\ g^{-1}$)	Cycle number	Initial capacity ($mAh\ g^{-1}$)	Reversible capacity ($mAh\ g^{-1}$)	Capacity retention (%)	Ref.
Coaxial MnO/C nanotubes	188.9	25	678.3	596	83.9	3
MnO/C nanoparticles	75	50	740	470	63.5	4
Interconnected porous MnO nanoflakes	246	100	568.7	648.3	114	5
Porous MnO microspheres	50	50	760	668.8	88	6
MnO/C core-shell nanorods	200	40	790	600	76	7
MnO/C nanocomposites	100	50	700	688.5	98.3	8
Nitrogen-doped MnO/graphene nanosheets	100	90	700	772	110.3	9
Porous MnO/C nanotubes	100	100	810.3	763.3	94.2	10
MnO@1-D carbon composites	1460	1000	300	810	270	11
MnO@C core-shell nanoplates	200	30	770	563	73.1	12
MnO/C composites	150	15	220	170	77.3	13
MnO@carbon core-shell nanowires	500	200	1036	801	77.3	14
Porous C-MnO disks	100	140	1387.2	1044.2	75.3	15
Mesoporous MnO/C networks	200	200	1456	1224	84	16
Hierarchical Micro/Nanostructured MnO	100	200	1051.4	782.8	74.4	17
Carbon-encapsulated MnO with N-doped carbon webs	100	700	1272	1284	101	18
MnO/graphite nanosheet	200	50	700	437	62.4	19
MnO/reduced graphene oxide sheet	100	50	700	665.5	95	20
Hollow porous MnO/C microspheres	Multiple rate (100 to 3000)	120	742	705	95	This work

References

3. Ding, Y. L.; Wu, C. Y.; Yu, H. M.; Xie, J.; Cao, G. S.; Zhu, T. J.; Zhao, X. B.; Zeng, Y. W. Coaxial MnO/C Nanotubes as Anodes for Lithium-Ion Batteries. *Electrochim. Acta* **2011**, *56*, 5844-5848.

4. Liu, Y. M.; Zhao, X. Y.; Li, F.; Xia, D. G. Facile Synthesis of MnO/C Anode Materials for Lithium-Ion Batteries. *Electrochim. Acta* **2011**, *56*, 6448-6452.

5. Li, X. W.; Li, D.; Qiao, L.; Wang, X. H.; Sun, X. L.; Wang, P.; He, D. Y. Interconnected Porous MnO Nanoflakes for High-Performance Lithium Ion Battery Anodes. *J. Mater. Chem.* **2012**, *22*, 9189-9194.

6. Zhong, K. F.; Zhang, B.; Luo, S. H.; Wen, W.; Li, H.; Huang, X. J.; Chen, L. Q. Investigation on Porous MnO Microsphere Anode for Lithium Ion Batteries. *J. Power Sources* **2011**, *196*, 6802-6808.

7. Sun, B.; Chen, Z. X.; Kim, H. S.; Ahn, H.; Wang, G. X. MnO/C Core-Shell Nanorods as High Capacity Anode Materials for Lithium-Ion Batteries. *J. Power Sources* **2011**, *196*, 3346-3349.

8. Liu, J.; Pan, Q. M. MnO/C Nanocomposites as High Capacity Anode Materials for Li-Ion Batteries. *Electrochem. Solid-State Lett.* **2010**, *13*, A139-A142.

9. Zhang, K. J.; Han, P. X.; Gu, L.; Zhang, L. X.; Liu, Z. H.; Kong, Q. S.; Zhang, C. J.; Dong, S. M.; Zhang, Z. Y.; Yao, J. H.; *et al.* Synthesis of Nitrogen-Doped MnO/Graphene Nanosheets Hybrid Material for Lithium Ion Batteries. *ACS Appl. Mater. Interfaces* **2012**, *4*, 658-664.

10. Xu, G. L.; Xu, Y. F.; Sun, H.; Fu, F.; Zheng, X. M.; Huang, L.; Li, J. T.; Yang, S. H.; Sun, S. G. Facile Synthesis of Porous MnO/C Nanotubes as a High Capacity Anode Material for Lithium Ion Batteries. *Chem. Commun.* **2012**, *48*, 8502-8504.

11. Li, X. N.; Zhu, Y. C.; Zhang, X.; Liang, J. W.; Qian, Y. T. MnO@1-D Carbon Composites from the Precursor $C_4H_4MnO_6$ and Their High-Performance in Lithium Batteries. *RSC Adv.* **2013**, *3*, 10001-10006.

12. Zhang, X.; Xing, Z.; Wang, L. L.; Zhu, Y. C.; Li, Q. W.; Liang, J. W.; Yu, Y.; Huang, T.; Tang, K. B.; Qian, Y. T.; *et al.* Synthesis of MnO@C Core-shell Nanoplates with Controllable Shell Thickness and Their Electrochemical Performance for Lithium-Ion Batteries. *J. Mater. Chem.* **2012**, *22*, 17864-17869.

13. Hao, Q.; Xu, L. Q.; Li, G. D.; Ju, Z. C.; Sun, C. H.; Ma, H. Y.; Qian, Y. T. Synthesis of MnO/C Composites Through a Solid State Reaction and Their Transformation into MnO_2 Nanorods. *J. Alloys Compd.* **2011**, *509*, 6217-6221.

14. Li, X. W.; Xiong, S. L.; Li, J. F.; Liang, X.; Wang, J. Z.; Bai, J.; Qian, Y. T. MnO@Carbon Core-Shell Nanowires as Stable High-Performance Anodes for Lithium-Ion Batteries. *Chem.*

– *Eur. J.* **2013**, DOI: 10.1002/chem.201203553.

15. Sun, Y. M.; Hu, X. L.; Luo, W.; Huang, Y. H. Porous Carbon-Modified MnO Disks Prepared by a Microwave-Polyol Process and Their Superior Lithium-Ion Storage Properties. *J. Mater. Chem.* **2012**, *22*, 19190-19195.

16. Luo, W.; Hu, X. L.; Sun, Y. M.; Huang, Y. H. Controlled Synthesis of Mesoporous MnO/C Networks by Microwave Irradiation and Their Enhanced Lithium-Storage Properties. *ACS Appl. Mater. Interfaces* **2013**, *5*, 1997-2003.

17. Xu, G. L.; Xu, Y. F.; Fang, J. C.; Fu, F.; Sun, H.; Huang, L.; Yang, S. H.; Sun, S. G. Facile Synthesis of Hierarchical Micro/Nanostructured MnO Material and Its Excellent Lithium Storage Property and High Performance as Anode in a MnO/$LiNi_{0.5}Mn_{1.5}O_{4-\delta}$ Lithium Ion Battery. *ACS Appl. Mater. Interfaces* **2013**, *5*, 6316-6323.

18. Chen, W. M.; Qie, L.; Shen, Y.; Sun, Y. M.; Yuan, L. X.; Hu, X. L.; Zhang, W. X.; Huang, Y. H. Superior Lithium Storage Performance in Nanoscaled MnO Promoted by N-Doped Carbon Webs. *Nano Energy* **2013**, *2*, 412-418.

19. Liu, S. Y.; Xie, J.; Zheng, Y. X.; Cao, G. S.; Zhu, T. J.; Zhao, X. B. Nanocrystal Manganese Oxide (Mn_3O_4, MnO) Anchored on Graphite Nanosheet with Improved Electrochemical Li-Storage Properties. *Electrochim. Acta* **2012**, *66*, 271-278.

20. Mai, Y. J.; Zhang, D.; Qiao, Y. Q.; Gu, C. D.; Wang, X. L.; Tu, J. P. MnO/Reduced Graphene Oxide Sheet Hybrid as An Anode for Li-Ion Batteries with Enhanced Lithium Storage Performance. *J. Power Sources* **2012**, *216*, 201-207.